Pedestrian lower limb injury criteria evaluation

A finite element approach

Pierre-Jean Arnoux* — Michel Behr* — Lionel Thollon*,**
Jérome Cardot* — Dominique Cesari* — Christian Brunet*

** Laboratoire de Biomécanique Appliquée, UMRT24 INRETS*
Université de la Méditerranée, Faculté de Médecine Nord,
Bd. Pierre Dramard, F-13916 Marseille
*** MECALOG Business Unit Safety, Faculté de Médecine Nord*
Bd. Pierre Dramard, F-13916 Marseille

pierre-jean.arnoux@inrets.fr

ABSTRACT. *In the field of pedestrian injury biomechanics, knees and lower legs are highly recruited during crash situations, leading to joint damage and bones failures. This paper shows how numerical simulation can be used to complete injury mechanism analysis and then to postulate on a knee injury criteria in lateral impact. It focuses on relationships between ultimate lateral bending and shearing at the knee level and potential ligament damage, based on subsystem experimental tests. These ultimate knee lateral bendings and shearings for potential failure of ligaments (posterior cruciate, medial collateral, cruciates and tibial collateral) were estimated at 16° and 15 mm in pure lateral shearing and bending impact tests respectively. Then this methodology was applied on a full test of pedestrian impact.*

RESUME. *Lors d'un choc piéton, les articulations des membres inférieurs, et en particulier les genoux subissent d'importantes sollicitations se traduisant par de l'endommagement et de la rupture pour les structures ligamentaires et osseuses. Cet article montre comment la simulation numérique peut être utilisée pour compléter l'analyse des mécanismes lésionnels et la mise en place de critères de blessure du genou en choc latéral. Il s'agit ici d'évaluer les relations entre le niveau de flexion ou de cisaillement latéral et l'endommagement potentiel des ligaments à partir d'essais expérimentaux sous systèmes. Les seuils de blessure en rotation latérale pure et en cisaillement latéral pur ont été estimés à 16° et 15 mm. Cette méthodologie est ensuite appliquée au cas d'un essai dit pleine échelle de choc piéton.*

KEYWORDS: *lower limb model, injury criteria, knee ligaments, pedestrian impact.*

MOTS-CLES : *modèle du membre pelvien, critère de blessure, ligaments du genou, choc piéton.*

REEF – 14/2005. Biomechanics of impact, pages 487 to 515

1. Introduction

In the field of biomechanics of impact and crashworthiness, safety concerns are always more linked to the notions of injury mechanisms, injury criteria or injury risks regarding one particular crash situation. This knowledge is also straight related to the improvement of safety systems evaluation means, wether it is for pedestrians, cyclists or car occupants. At a research level, and to begin with injury mechanisms understanding, we need to define injury criteria correlated to trauma situations. This is why both experimental and numerical approaches have been used to investigate the human behaviour and tolerance under impacts and to develop realistic human body models (Nyquist *et al.* 1985, Kajzer *et al.* 1993, Crandall *et al.* 1996, Parenteau 1996, Lizee *et al.* 1998, Atkinson *et al.* 1998, Thollon *et al.* 2001, Behr *et al.* 2001, Arnoux *et al.* 2001, Beillas *et al.* 2001).

Lower limbs are highly loaded during crash situations (AIS from 2 to 6) with joints damages and bones failures (Stutts 1999, IHRA 2000). From an experimental point of view, during a pedestrian impact, knee injuries could result from a combination of lateral shearing and bending of the knee (Kajzer 1990, Kajzer 1993, Grzegorz 2001, Bose 2004). On cadavers full leg experiments, Kajzer (1990 & 1993) focused on impact forces and bending moment corridors. He showed that pure shearing induces collateral tibial and anterior cruciate ligaments failure while a primarily bending mainly induces medial collateral ligament failure. More recently, Bose (2004) performed 3-point bending tests on isolated knee joints in order to obtain a combination of shearing and bending effects, and confirmed injuries to medial collateral and anterior cruciate ligaments. It can be noted that knee injuries are not restricted to the injuries described above. Tibia fractures (especially with at the tibial eminence in contact with the intercondylar notch at impact), posterior cruciate ligament injuries, fibula and femur fractures can also be observed. From all these studies, it appears that the main challenge for improving leg protection should focus on knee ligament damage and failure minimization.

In order to more accurately describe the injury mechanisms involved in such trauma situations, finite element simulations (once the model validated through experimental tests) can be performed and require always finer models of the human body. In the literature, many finite element models have been designed to study very specific points of the leg behaviour under crash situations. Some ankle-foot models focused on the kinematics (M. Beaugonin *et al.* 1996, P. Beillas *et al.* 1999), others on material properties (M. Beaugonin *et al.* 1997, R. Tannous *et al.* 1996) and others else on an accurate description of geometry (P. Beillas *et al.* 1999). Knee models were also developed both for frontal impacts (S. Hayashi *et al.* 1996, P. Atkinson 1998) and pedestrians (J. Yang 1997, P. Schuster *et al.* 2000). Lastly, Bedewi (1996) included mathematical joints in order to control the kinematics of a full lower limb model. The THUMS model (Chawla 2004) or the LLMS model (lower limb model for safety, illustrated in Figure 1), designed in collaboration between Mecalog and the “Laboratoire de Biomécanique Appliquée”, are advanced finite element models of the whole lower limb (Arnoux 2001, 2002, 2003, 2004, Beillas 2001). This last

model was based on an accurate description of all anatomical parts of the lower limb, and its validation was performed in various impact situations (isolated materials, sub-segments up to the whole model).

One major interest in human modelling lies in the possibility of numerically recording specific parameters (strain, stress, pressures and kinematics) that are not approachable in experiments. With such data, it becomes easier to show tissue kinematics and mechanical behaviour during the crash chronology and then to postulate on potential injuries. For knee injuries on pedestrians, one way to define an injury risk criterion or an injury probability for knee soft tissues is to evaluate the ultimate lateral bending and shearing levels of the knee before damage, when the impact occurs. In order to investigate the corresponding injury mechanisms and then evaluate these ultimate levels, we have used the LLMS finite element model of the lower limb.

This paper gives a general overview of the model, from geometry acquisition (based on MRI and CT-scan data) to the modelling choices and validation database. Then, a specific analysis of the model response (bone von Mises stress levels, ligament global and local strain levels, knee rotation and shearing measurements) was performed. These numerical simulations are based on previous experimental work reported by Kajzer (1990 & 1993). It consists in lateral bending impact tests on an isolated lower limb (the impact being applied on the internal malleolus); then, a pure shearing impact test on an isolated lower limb was performed, the tibia being loaded simultaneously at its two extremities. As impact velocity in pedestrian is a gravity factor, this first test campaign was focused on extended velocities ranging from 2 to 10 m/s.

2. Model design and validation

2.1. *Mesh definition*

The model geometry was obtained on a human male volunteer close to the 50^{th} percentile. Measurements were performed in the sagittal plane from the hip to the toe region (the leg being extended). The scanning step was set to 1 mm in joint regions and ranged from 5 to 10 mm in other regions. Moreover, longitudinal and frontal images taken between the femur and the tibia were used in order to determine the geometry of the menisci, to check hip connections in the pelvis area and more generally to check images alignments. Altogether, more than 600 images (approximately 150 CT scans and 460 MRI images) were available for the reconstruction of the model geometry.

Once MRI measurements were achieved, each anatomical component was identified by anatomists on each section. The contours were then computed to create a 3D reconstruction of the lower limb (figure 1). It was then possible to mesh all parts of the model using shells, membranes, bricks and other solid elements depending on the modelled parts. For this purpose, two main methods can be used,

the first consisting in decomposing geometrical entities in a set of splines which were meshed separately and assembled (with an offset to obtain solid mesh); the second method consists in using specific algorithms (Bidal 2003) to directly generate 2D meshes. Due to the cortical bones thickness and the time step constraint, compact bones were modelled using shell elements. The inner and outer cortical surfaces were used to compute a mid-surface and to estimate the bone local thickness at each section.

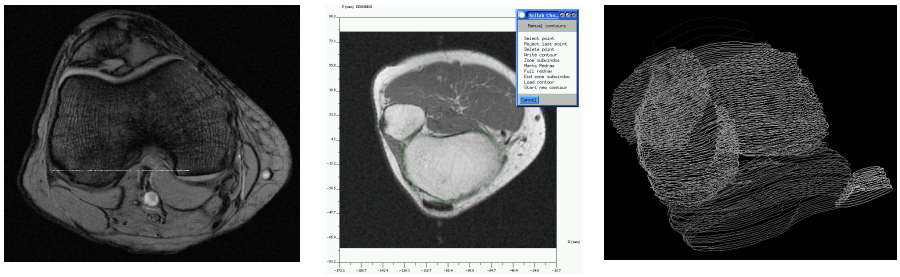

Figure 1. *Computation of RMI data to obtain 3D contours of anatomical parts*

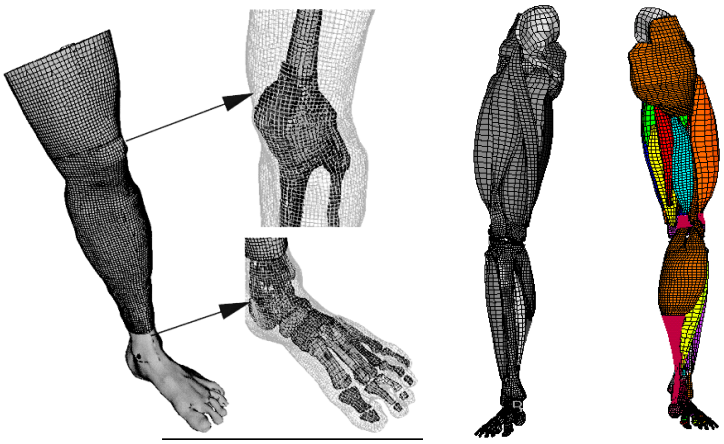

Figure 2. *Model overview: gathered flesh version (left) and tonic version (right)*

According to the level of refinement, the model includes approximately 28000 elements in its first version, 35000 in the flesh refined version and up to 90000 in the tonic muscles version (figure 2). The model includes all structures which have a contribution to the mechanical behaviour of the lower limb *i. e.* compact and trabecular bones, knee cartilage, menisci, knee ligaments, ankle foot ligaments, tendons membranes, muscles and skin. Muscle description was multiple. One

solution was based on gathering passive muscles in one same volumic part called flesh (figure 1) using bricks elements. Another solution was based on meshing all muscles bundles separately, taking into account their active properties with mixed meshes (including shells, active springs and passive brick elements) (Behr 2003).

Starting from the analysis of MRI measurements and from anthropometric considerations, the long bones were segmented in several geometrical parts in order to take bone thickness and density distribution into account on the different regions of the bones (as illustrated in figure 3).

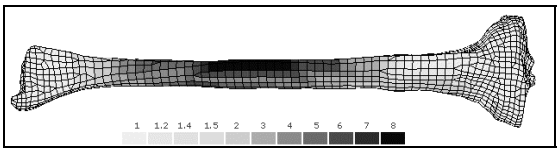

Figure 3. *Example of thickness distribution along tibia*

Table 1. *Type of elements used in the lower limb model. Note that "spg" was an abbreviation of spring and "dof" for degree of freedom*

	Spg 1dof	Spg 6dof	Shell	brick
Compact bones			y	
Spngious bones				y
Cartilages				y
Knee cruciates ligaments			y	y
Others knee ligaments	y		y	
ankle-foot ligaments			y	
Phalanx ligaments		y		
Membranes			y	
Meniscus				y
Tendons			y	y
Muscles / Flesh	y		y	y
Skin			y	

The model includes three main types of meshes:

– The solid mesh i.e brick elements are 8 nodes lumped mass formulation isoperimetric elements. The solver being an explicit code, reduced integration scheme was used with (in most of case) a Belytschko hourglass control.

– The shell elements are (Q4) bilinear Mindlin plate elements coupled with a reduced integration scheme using one integration point and a Belytschko Hourglass mode.

– One degree or 6 degrees of freedom spring elements which can include viscoelastic behaviour (through spring and dashpot in parallel) or user-defined stiffness functions.

An overview of elements types used for the different structures in the model is reported in table 1. As this paper focus on knee joint injuries, a more detailed description of knee joint mesh is proposed in appendix 1.

2.2. *The model: from material definition to interface modelling*

Compact and spongious bones were modelled with a Johnson Cook elasto-plastic material law. It is established that material and geometrical properties of biological tissues, especially bones changes according to the considered region. Compact bone thickness can exhibit variation on a same slice and also according to the location along the bone. If on diaphysis, this thickness is important, it decreases near the metaphysis and becomes very thin on the epiphysis. At the opposite, spongious bone proportion is preponderant on bone extremity and very low in diaphysis. These variations also induce differences in bone densities and consequently on material properties (Young's modulus and Yield stress). According to the literature data, different sets of parameters were used for each bone (Burstein 1972, Goldstein 1987, Reilly 1975, McElhaney 1966). Property variations on the same bone were included (considering differences and transitions between diaphysis, epiphysis or metaphysis) and were defined as mean value according to literature data analysis. Foot bones (the 5 metatarsis, the 5 phalanx, the 3 cunei and the cuboid) were set rigid. Mechanical parameters of bones are summarized in table 2. Solid spongious elements and their surrounding shell meshes (for compact bones) are not coincident. They were connected in the model using tied contact interfaces.

Table 2. *Summary of elastoplastic properties of bones*

	Compact	**Spongious**
Young Modulus	9-15 Gpa	10-450 Mpa
Poisson ratio	0.3	0.3
Yield stress	80-120 Mpa	10 MPa
Ultimate stress	110-130 Mpa	15MPa
Hardening (param & coef)	100Mpa - 0.1	100Mpa - 0.1
Ultimate strain	2-3 %	3%

Foot-ankle ligaments and Achille's tendon were modelled using viscoelastic shells and/or springs. Each fibre includes several springs in order to describe the contact interface between ligaments and their external surface. Cruciate ligaments and patellar tendon were described using both solids and shells in order to model

membranes around the structure. Negligible stiffness 2 to 5mm long springs were also added along the main axis of ligaments in order to record deformations. As they were described as a thickening of knee capsula, lateral ligaments and patellar wings were described using shell elements. Lastly, fibular-tibial ligaments and meniscus ligaments were described using springs. Knee Ligaments and tendons were modelled with a generalized viscoelastic Kelvin Voigt material law or using elastic or viscoelastic spring elements based on literature data (Arnoux 2000, Johnson 1996, Noyes 1976, Attarian *et al.* 1985) (Table 3). Cartilage and menisci, which contribute to an accurate control and a good stability of the knee joint during motion, were modelled using elastic solid elements (Appendix 1). This biphasic material (incompressible fluid within a fibrous structure) is highly strain rate dependent. The mechanical properties of such a structure are strongly related to fluid exudation effects during loading. In this study, and due to the dynamic loading condition, we assumed, in a first approximation, the material being elastic (with a Young's modulus of 20 MPa based on results of Yamada 1970, Repo 1977, and Atkinson 1998) in order to take the effects of strain rates into account. Same assumptions were formulated for meniscus with a Young modulus of 200MPa, also considering the structural differences with cartilages (Mow *et al.* 1992, Li *et al.* 2003, Yamada 1970, Radin *et al.*1970). Because of the lack of data on its dynamic properties, the capsula was described as an elastic material using shell elements (with a Young's modulus of 20 MPa). In the considered model version, muscles were modelled in two separate ways. Firstly, the muscles action lines are described using springs elements (passive). Secondly, muscles bodies are modelled using solid elements in order to give a unique volumic shape to muscles and other aponevrotic tissues, and to describe damping properties during shocks. Except for foot phalanx joint described with a mathematical joint, all joints are defined using anatomical components that contribute to joint kinematics and stability. Therefore, and in order to ensure interaction between tissues, several interfaces were defined:

1) Bones to bones, bones to ligaments and ligaments to ligaments. Cartilages to cartilage interfaces are also introduced to describe joints or moving tissue contacts. They are modelled using self contact interfaces and edge to edge contact interfaces.

2) Tied contact interfaces, which ensure attachments (spongious bone to compact bone, flesh to bones), were modelled.

Table 3. *Summary of viscoelastic properties of ligaments*

	Ligaments & tendons
Young modulus	50-225 Mpa
Poisson ratio	0,3
Tengent Young modulus	48-155 Mpa
Tengent Poisson ratio	0,37
Viscosity in pure shear	6,6

2.3. *Model validation*

As this model validation has already been presented in previously published papers (Arnoux 2001, 2002, Arnoux 2004, Beillas 2001), we only focuse here on lateral impact tests performed on the lower limb which are at the origin of our methodology to determine injury criteria. The lower limb model validation was performed at different levels:

1. The mechanical properties of isolated tissues were checked under traction tests on isolated knee ligaments, patellar tendon and Achille's tendon (Arnoux 2002, Johnson 1994, Haut 1990). These tests consisted in checking the force versus time or force versus deformation curves regarding the experimental corridor. Note that failure properties were not integrated at this stage in the model. During the loading test, it was also possible to show stress distribution in the ligaments structure. Localization of high stress levels in the neighbouring of bone insertions was relevant with failure profiles observed during the experimental tests. Properties of passive muscles were checked under compression testing as it has been done during the Humos project (Behr 2003). The bones structure were tested mainly using three point bending tests (Hayashi 1996, Beillas 1999).

2. The second level was illustrated with the model ability to describe knee passive flexion (gravity loading). Kinematics were checked by anatomists focusing on the combined sliding and rolling movement of the femur on the proximal tibia. The sliding of the patella between the two femoral condyles and the action of the ligaments linked to the patella were checked; The interaction between the two cruciate ligaments during flexion and, at last, the contribution of meniscus to ensure a correct contact interface between bones were also checked. Note that in the tonic version of the model (Behr 2003) it was possible, by muscles bracing simulations, to obtain relevant kinematics of the three joints of the lower limb (hip, knee and ankle foot).

3. The third validation level deals with sub segment testing in order to evaluate the structure behaviour including soft and hard tissues. Various tests were performed at this stage (see Appendix 2). Concerning lateral impact situations, Nyquist tests (Nyquist 1985) which consisted in performing 3-point bendings were included in the validation database. The computed bending torque was found within the experimental corridor, with 360 Nm in lateral medial flexion (experimental data ranging from 241 to 419 Nm) and 297 Nm in anterior posterior flexion (experimental corridor ranging from 214 to 394 Nm).

4. The whole model validation was obtained by frontal and lateral crash simulations in order to identify complete injury mechanisms. The lateral bending impact test was performed in order to identify the mechanism of one of the main injury occurring in pedestrian impacts (J. Kajzer *et al.* 1990, J. Kajzer *et al.* 1993). In these tests, the upper leg was allowed to freely translate in the vertical direction, while a 22 kg dead weight was attached to the proximal femur to simulate the weight of the body. The foot was placed on a plate which allowed free translation along the

direction of impact. A 40 kg impactor was used to load the distal tibia with an impact velocity of 20 Kph (figure 4). The model validation was performed by comparing forces versus time recorded on the impactor face. Results were found within the experimental corridors build with 15 experimental tests (figure 4).

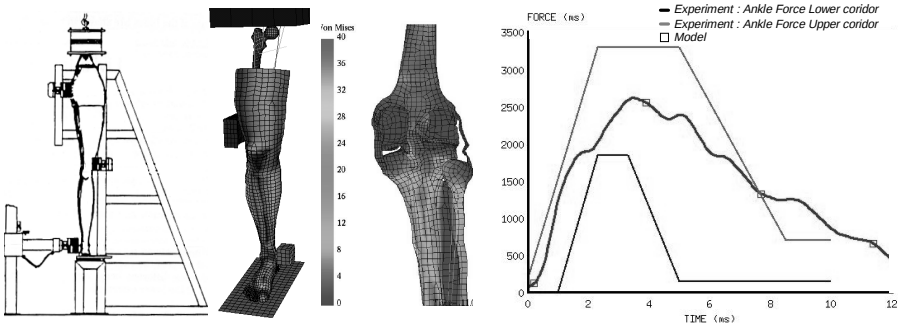

Figure 4. *Test set up for lateral lower limb bending tests. Force vs time curve on the ankle impactor. Von Mises stress at 0 and 11 ms*

For the shearing tests, the impactor had two impacting surfaces simultaneously applied on both proximal and distal extremities of fibula and tibia (figure 6). The knee impact force versus time curve showed two different injury mechanisms. The first injury mechanism which can be directly related to the knee impact force (for example head of fibula failure, or extra articular fracture) occurred after approximately 5 ms and was identified as the first peak on the force versus displacement curve. The second injury mechanism was correlated to the force transmitted through the knee joint during the impact. This phenomenon was identified by the relative displacement of the tibia which produces injuries in the neighbouring ligaments. The resulting impacting forces predicted by the leg model were relevant with the experimental corridor build with 19 experimental tests (figure 5). Nevertheless, the two-stage injury mechanisms experimentally identified, with the two peaks in the force time curve, was not reproduced with the LLMS model. In the case of a shearing impact, the injury mechanism is very complex and follows two steps. The first injury mechanism, which occurred 5 ms after impact, is directly related to the knee impact force. It can be described as a contact injury and can induce bone fractures (head of fibula, tibia or femur). The second injury mechanism is correlated to forces transferred through the knee during acceleration of the thigh (relative shearing of tibia versus femur) which lead to soft tissues injuries. This could be linked to soft tissue behaviour laws where physical failure was not implemented in the model. However, the locations of stress concentrations predicted by the model, including the cruciate ligament insertions, the tibia eminence and the tibia fibular joint, were in agreement with the injury locations found during the autopsies (Figure 5).

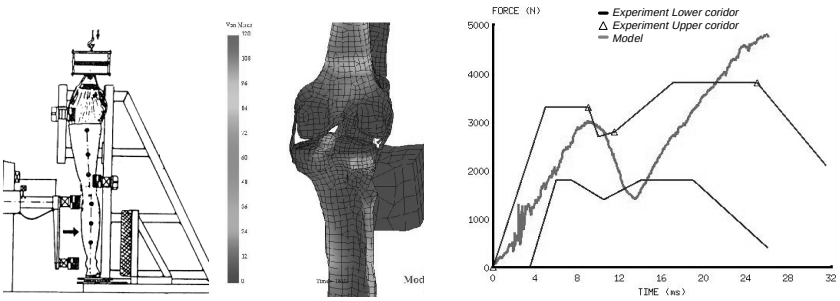

Figure 5. *Overview of testing conditions, Impact force versus time and von Mises stress concentrations on the knee during impact*

For these two tests, the deformation levels were recorded on each ligament and used to postulate on potential injuries. This point is detailed in the next part of the paper.

3. Injury criteria evaluation

3.1. *Methods*

Once the finite element model was assumed to be validated, by taking care to the validity domain, loading cases can be extended and, from model analysis, it remains possible to compute data that is not usually recordable experimentally. It concerns stress distribution, strain levels, pressure or specific displacements. Therefore, the link between new recorded data and test chronology can help to improve injury mechanisms description and then to postulate on injury criteria. This methodology (Tropiano 2004, Thollon 2002) was adapted in this study to the following points:

– *Kinematics interpretation.* Kinematics are recorded in order to check the global behaviour of the model and to study its interactions with the environment. In the LLMS model, this kinematics can also be recorded at each joint in order to check the correct relative movements between the corresponding bones or soft tissues. It gives, in a first approximation, information about the global kinematics behaviour (in lateral bending, in flexion – extension, in rotation or during combined motions) in order to validate the correct function of joints. In this work, we specifically focused on the relative rotation between tibia and femur bones. By computing the scalar product between femoral and tibial axes (frontal and antero-posterior), it was possible to calculate knee torsion, lateral bending and frontal bending in the different planes and for each test. Therefore, concerning shearing, the lateral relative displacement between the tibial eminence and the intercondylar notch was calculated to accurately identify knee lateral shearing at the joint level.

– *The force and stress level.* The force, and more particularly the stress level and distribution in bones (against time) can be studied in order to evaluate the location and evolution of hard tissues injuries. Due to the mechanical properties of bones, damage is assumed to occur on bone structures when stress reaches the Yield stress values. The different von Mises stress levels obtained with the model are compared to the Yield and ultimate stress levels implemented in the different sets of parameters of the compact bone.

–- *Strain measurements* can be mainly attributed to soft tissue injury evaluation. Damage properties of soft tissues can be described in terms of ultimate strain levels in soft tissue structures. In the particular case of the knee ligaments, a previous experimental work (Arnoux 2000, 2002) produced the mechanical properties of knee ligaments under dynamic loadings, up to their complete failure . The results led to consider ligament failure with a strain criterion. Ultimate strain levels were calculated for the four knee ligaments and used in this study to identify potential failure. Note that literature gives various values for ultimate strain (Table 4) obtained in different experimental conditions (loading, preconditioning, conservation method…).

Table 4. *Overview of ultimate strain levels recorded for knee ligaments*

Author	Collateral tibial	Collateral medial	Posterior cruciate	Anterior cruciate
Viidick (1973)	30%	40%	60%	60%
Kennedy (1976)			24 (+/- 6) %	
Marinozzi (1982)			20 (+/- 5) %	
Prietto (1992)			28 (+/- 9) %	
Race (1994)			18 (+/- 5)	
Arnoux (2000)	24-38%	22-38%	15-23%	18-24%
Kerrigan (2003)	7-10%	11-20%		

In the field of pedestrian impact, two injury mechanisms were described at the knee level, *i.e.;* pure lateral shearing of femur relative to tibia and pure lateral bending between tibia and femur. In order to postulate on injury criteria through injury mechanisms analysis, we decided to first focus on experimental testing for which injury mechanisms were dissociated. Then numerical experiments consisted first in lateral bending impact tests on an isolated lower limb (the impact being applied on the internal malleolus). A pure shearing impact test on an isolated lower limb was also performed (the tibia being loaded simultaneously at its two extremities).

For each of the four knee ligaments, strain sensors were inserted in the model. These sensors consist in a series of springs (with initial length between 4 & 9mm)

along the main fiber axis as previously mentioned. For the cruciate and lateral ligaments, it was also possible to compute the global strain level, the average strain level as well as the curve of maximum strain recorded at various levels in the ligament. These computed strain levels are then compared to the experimental ultimate strain levels (Table 4) in order to postulate on a potential failure of the ligaments during the simulation. The same experiments as those described in the model validation chapter were used. The impact velocities chosen for these studies are 2 m/s, 4 m/s, 5.55 m/s, 7 m/s and 10 m/s. The typical impact force recorded on the impactor during each test (and reported in figure 6) gives an overview of the velocity influence on numerical simulations.

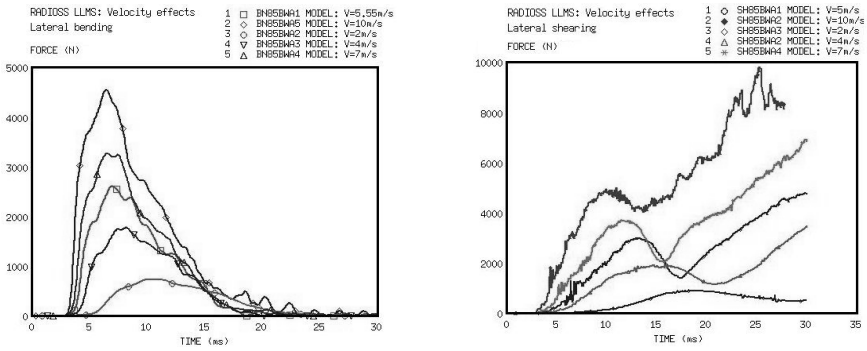

Figure 6. *Impact forces recorded on medial ankle versus time for the five impact velocities in bending tests (left). Impact force recorded on the upper bumper during the shearing test (right)*

3.2. *Analysis of stress distribution curves*

The von Mises stress levels on bones were located on the proximal tibial metaphysis and distal femoral metaphysis (Figure 7) for both impact situations. For bending tests, the maximum von Mises stress level stays lower than the failure level and reaches 30 MPa at 2 m/s, 60 MPa at 4 m/s, 70 MPa at 5.55 m/s, 90 MPa at 7 m/s and 125 MPa at 10 m/s (which is close to the limit of failure). Note that stress concentration was also observed on ligament insertions (with lower values than those reported upwards). For shearing tests, the bones von Mises levels are higher. They reach 60 MPa at 2 m/s, 93 MPa at 4 m/s, 115 MPa at 5.55 m/s, 120 MPa at 7 m/s and 130 MPa at 10 m/s (with tibia failure). Stress concentrations were observed at the contact area between proximal fibula and tibia (and may be produced by the contact with the impactor), at the tibial eminence in contact with the intercondylar notch and with lower levels on ligaments insertions.

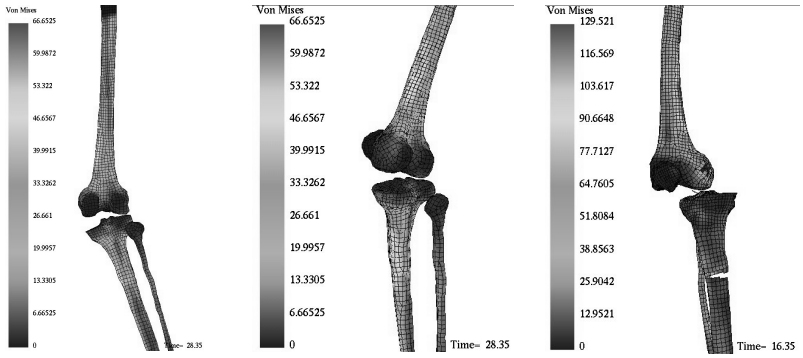

Figure 7. *Von Mises stress on bones for bending (V_0=5.55 m/s) and shearing impact (V_0=10 m/s)*

3.3. *Analysis of model kinematics*

For bending tests (Figure 8), the typical lateral rotation between the tibia and the femur was recorded with a rotation axis that seems to pass through the contact area between the femoral external condyle and the tibial external glena. The frontal rotation is stable with a variation ranging from 1° to 3° (figure 9), depending on the impact velocity. The torsion effect seems to be important and correlated to the impact velocity (Figure 8). Variations of angles reach values ranging from 2° to 8°, depending on the impact velocity. This point has to be linked to the asymmetrical geometry of the femoral condyle and the tibial glena. From a medical point of view, this torsion effect is described as a natural safety countermeasure of the human body during trauma situations in order to avoid (or limit) damage to ligaments. Lastly, lateral shearing effects could be neglected for this test (figure 9).

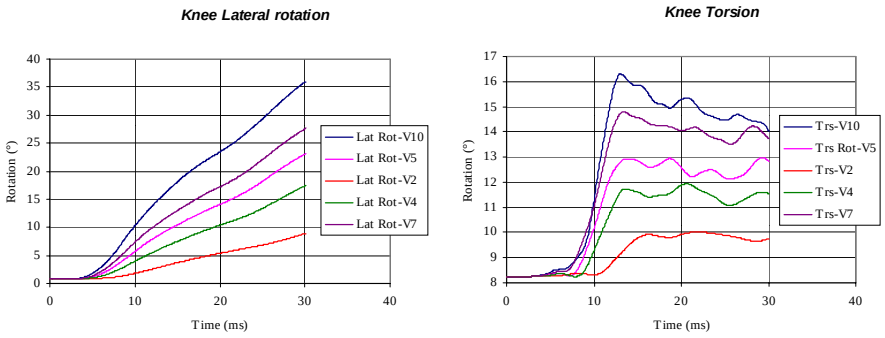

Figure 8. *Knee lateral rotation and knee torsion (along leg axes) in the bending test*

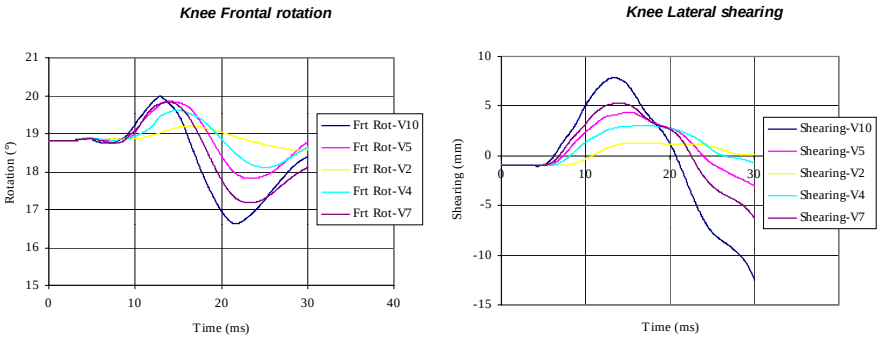

Figure 9. *Knee frontal rotation and knee lateral shearing in the bending test*

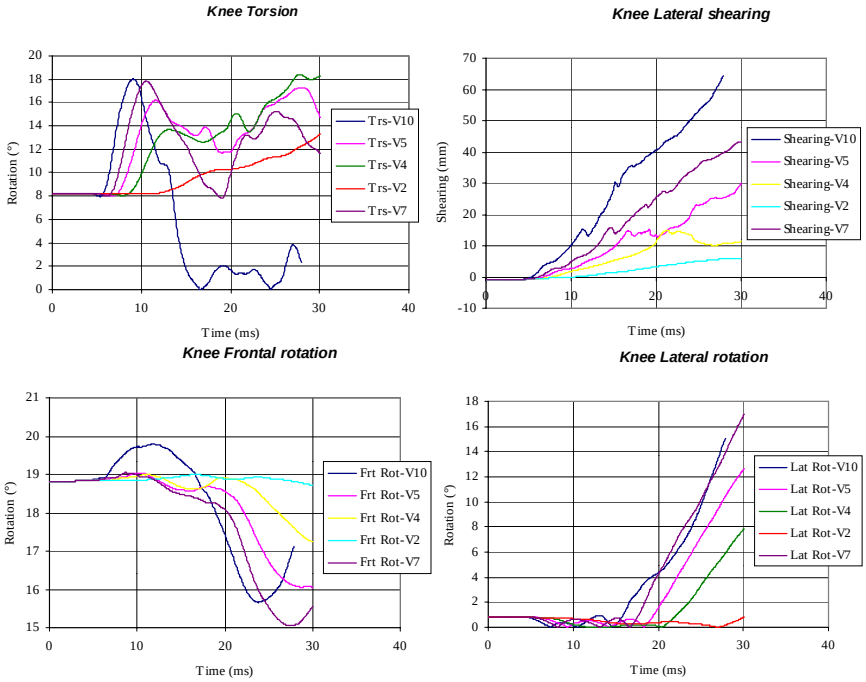

Figure 10. *Knee torsion and knee lateral shearing in the shearing test; Knee frontal rotation and knee lateral rotation in the shearing test*

For shearing tests, the two main kinematics aspects are the lateral shearing and the knee torsion (figure 10). The lateral shearing seems to be correlated with velocity and rapidly reaches high values which are not relevant with geometrical characteristics of the proximal tibia and distal femur. At 15mm of shearing the

curves reach a steady state which could result from the contact between intercondylar notch and tibia eminence. In the first 15 ms, the knee torsion reaches amplitudes ranging from 2° to 10° depending on the impact velocity (figure 10). These results showed that for these two loading modes the "natural safety systems" were active. The lateral rotation was low in the first phase of the test and then increased significantly (figure 10). Lastly the frontal rotation showed same variation levels as in the bending case (figure 10).

3.4. *Strain level analysis*

The strain level recorded on each ligament (cruciate and lateral) and correlated to rotation or shearing effects were computed in two ways:

1) The total strain in the ligaments is obtained by summing up the deflections recorded at each level of the ligament. This gives a general overview of the global strain within the structure.

2) The maximum strain in the ligaments is obtained with the maximum strain recorded at the different levels of the ligament. This strain gauge is used to locate high strain levels in the structure which could lead to damage or failure.

As previously mentioned, the implemented soft tissue behaviour laws do not take into account damage and failure mechanisms. In order to postulate on damage in the structure, our analysis was based on strain levels recorded in the ligaments and compared to ultimate strain level at failure, reported in a previously published experimental study (Arnoux 2002 & 2003). In the present study, the ultimate values used to postulate on damage were assumed to be 28% for lateral ligaments, and 22% for cruciate ligaments. Then, maximum strain can be considered as a first sensor to locate damage in the structure whereas the total strain gives a global overview of the whole structure. If the maximum strain reaches the ultimate strain level as defined above, we assume that damage can occur in the ligament. Moreover, if the ultimate strain level is reached on the total strain curve, the ligament failure can be postulated with a high probability.

For lateral bending tests, the lateral medial and the posterior cruciate ligaments were highly loaded. The strain versus time curve shows a strong sensitivity to impact velocity (figure 11). On the opposite, strain versus lateral bending seems to be independent of impact velocity (figure 11). A small difference between maximum strain level and total strain level seems to show that the medial collateral ligament in the model has homogeneous strain distribution. The maximum strain or total strain level used to postulate on damage in the ligaments is obtained with a lateral rotation ranging from 20 ° to 24 °. Concerning the posterior cruciate ligament, there is a strong difference between global strain (maximum strain) and local strain (maximum strain) which seems to show that local high strain levels were obtained. These observations are also observed through von Mises stress curves and seem to be relevant with experimental failure profiles during isolated traction tests of the

ligaments (Arnoux 2004, Subit 2004). Local damage could occur for knee rotation between 12 ° and 15 °, whereas global damage for knee lateral rotations was close to 26 ° (which seems to be very high). The strain level on the anterior cruciate and collateral tibial ligaments did not reach the injury level during the tests. From the first part of the strain versus time curves, the strain rate levels for each impact tests were evaluated on injured knee ligaments (figure 11). The strain rate curve seems to be a linear function of the impact velocity (figure 12). Significant differences were observed between the posterior cruciate and the medial collateral ligament, but also on a same ligament through total strain and maximum strain curves.

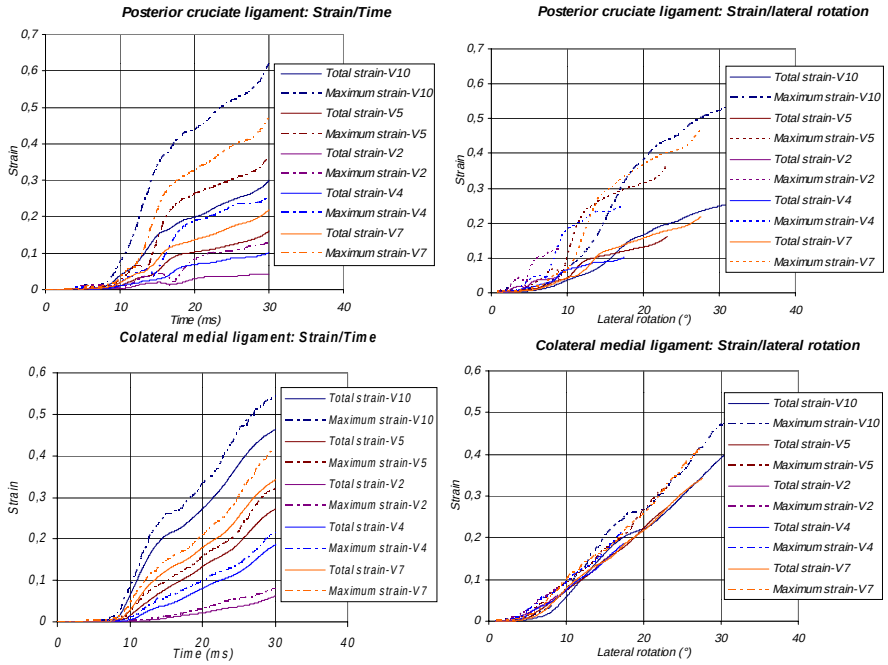

Figure 11. *Collateral medial ligament total and maximum strain curves versus time and versus lateral rotation; Posterior cruciate ligament total and maximum strain curves versus time and versus lateral rotation*

For the shearing tests, the two cruciate and the tibial collateral ligaments were highly loaded (Figure 13). As it was observed in bending tests, the effects of impact velocity were significant on strain versus time curves and had no effects on strain versus knee shearing curves. The small dispersion observed between total strain and maximum strain seems to indicate that strain is homogeneous in the anterior cruciate ligaments. The failure or damage could start at a 13 to 15 mm knee shearing. For the posterior cruciate ligament, the strain being not homogeneous on the structure, only

maximum strain levels were computed, and they show that damage could occur for shear values ranging from 12 to 14 mm. Finally, for the collateral tibial ligament, the maximum strain reaches up to 14-17mm according to the impact velocity.

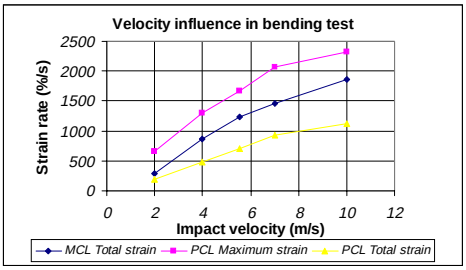

Figure 12. *Strain rate versus impact velocity curves on posterior cruciate ligaments (for total and maximum strain) and on collateral medial ligaments*

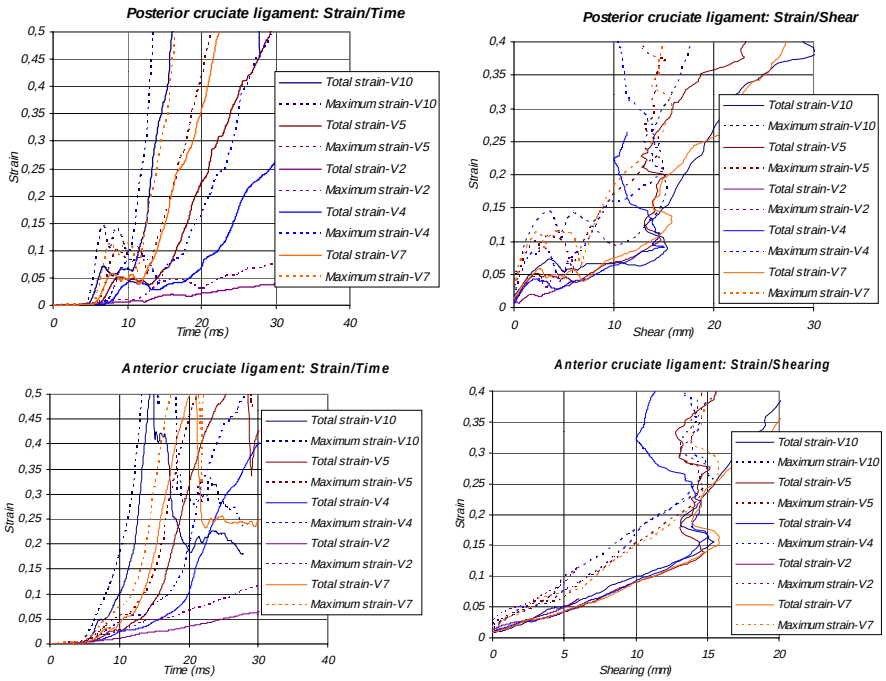

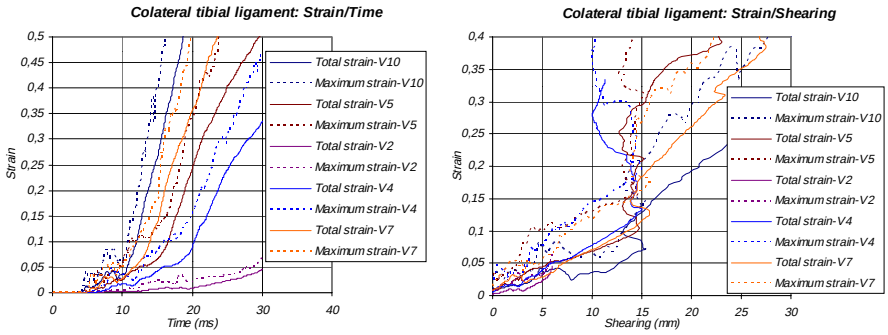

Figure 13. *Total and maximum strain curves versus time and versus lateral shearing for the posterior cruciate ligament, the anterior cruciate ligament and the collateral tibial ligament*

As it was performed for the bending impact test, the strain rate curves versus impact velocity were evaluated for the three injured ligaments. The same observation concerning the linear relation between velocities and dispersions in results are observed. Nevertheless, it appears that strain rate levels were higher in the shearing case (figure 14). This could be linked to a higher intensity in shock which could be induced by an impact applied close to the knee joint compared to the bending case.

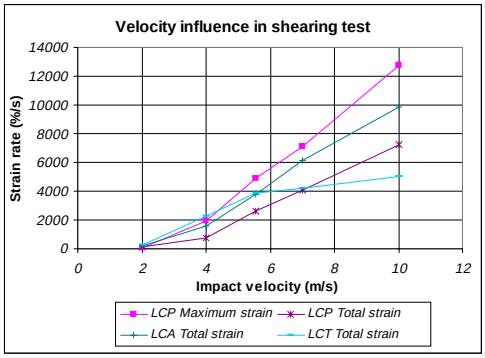

Figure 14. *Strain rate versus impact velocity curves on posterior cruciate ligaments (for total and maximum strain, the anterior cruciate ligament and on collateral medial ligaments)*

4. Application to a full scale pedestrian impact simulation

In the context of a French APPA (“Amélioration de la protection des piétons lors de collisions avec des automobiles”) PREDIT (“Programme de recherche et

d'inovation dans les transports terrestres") project, experimental coupled with FE simulation studies have been performed in order to improve knowledge on lower limb injuries mechanisms and criteria in the context of a pedestrian impact situation.

An experimental and numerical full scale test was performed. The test consisted of a 50 percentile post mortem human subject (PMHS, 1m75, 67Kg) obtained through the faculty of medicine of Marseille. The PMHS was preserved with Winckler solution, instrumented and put in conditions of a pedestrian impact. Note that details of this experiment were not reported in this paper. With this test, for which it was possible to check the methodology reported in this paper. The numerical test consisted first in coupling the lower limb model to an Hybrid III 50 percentile rigid dummy model in order to take into account the effects of the hole human body kinematics during the test. The coupling consisted in adding a part of the pelvis, and modifying the initial geometry of the dummy. The hip joint was then defined using a mathematical joint with user-defined functions for its six degrees of freedom. Note that during this work, we focus only on lower limb behaviour.

The model was then put in standing position in front of the car model with a light knee flexion and same height of the knee joint in front of the car bumper as those set in experiments (figure 15). The deformable car front was then put in braking conditions with an initial velocity of 10.88ms^{-1} and, according to the acceleration recorded during experiments, we postulated a constant deceleration of 5.58 ms^{-2}.

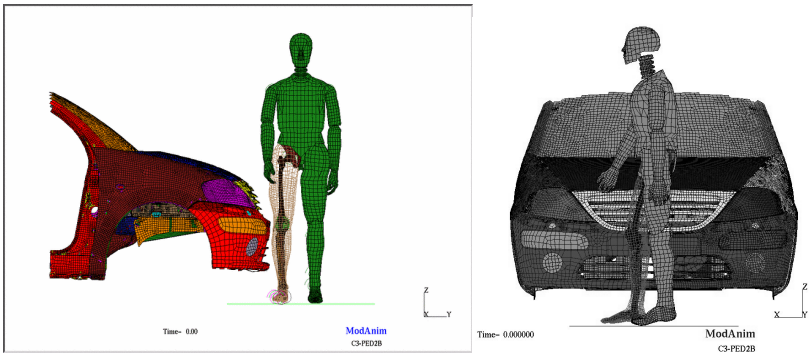

Figure 15. *Lateral and frontal view of the pedestrian impact situation*

The model kinematics (figure 16) were relevant with experimental ones recorded with high speed cameras (1000 frame per seconds). From the analysis of rotation and lateral shearing of the knee, we observed a strong lateral rotation effects (more than 15°) but a very small lateral shearing (lower than 5 mm). Note that in this case, torsion effects of the knee were also observed with same levels as those recorded for bending and shearing tests.

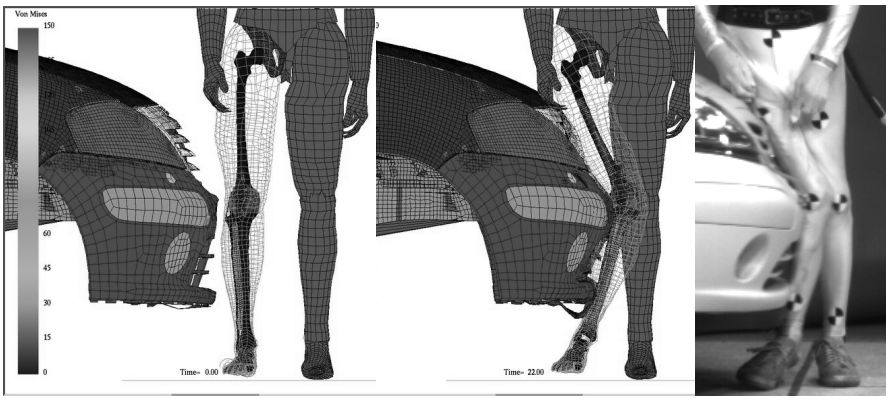

Figure 16. *Lateral and frontal view of the pedestrian impact situation*

From von Mises distribution, it was observed failure of the proximal fibula due to the contact with the bumper. No femur or tibia failure was reported, but von Mises distribution and amplitude were at the same level as those obtained with high speed bending and shearing tests (figure 17). Lastly strain versus time (figure 17) with same failure criteria as those used above showed failure of the posterior cruciate ligament, then of the medial collateral ligament and lastly of the anterior cruciate ligament (figure 17). The level of rotation as damage criteria was assumed to start on the maximal strain curves and was relevant to the 15° of lateral rotation obtained on previous simulations. It confirmed on a real impact configuration the injury criteria evaluated on the sub segment testings.

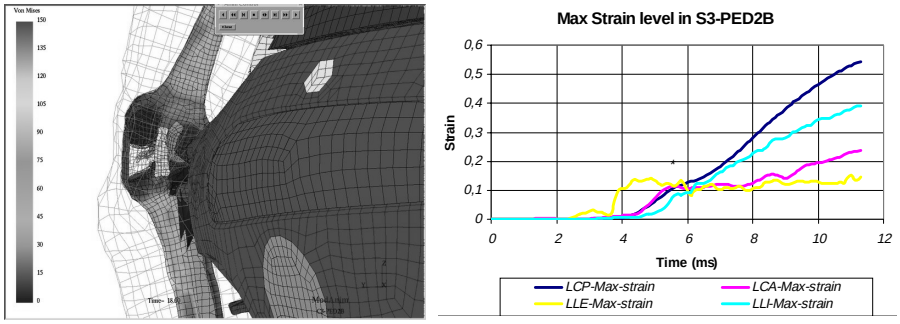

Figure 17. *Lateral view of the pedestrian impact situation*

5. Discussion. Conclusion

The objective of this work was to show how it is possible, when using an advanced FE model of the lower limb and numerical simulations at various impact

velocities, to improve injury mechanisms knowledge and to evaluate ultimate bending and shearing levels. Once these injury criteria were evaluated, these results were also applied to real crash situations by comparison to a representative full scale pedestrian impact.

5.1. *About the initial model*

The Lower Limb Model for Safety has been designed and validated to be able to describe multiple loading configurations. The accuracy obtained through the model geometry and mesh ensures a proper description of tissues interactions (through contacts definitions). Nevertheless these choices imply to include multiple types of interfaces in order to avoid penetrations and keep the stability and accuracy of the calculation. It concerns typical contact interfaces with coulomb friction which were defined as symmetrical and also specific edge to edge interfaces for which slave nodes and master surfaces were replaced by slave and master edges. This work has also showed that knee joint modelling can not be limited to the four main knee ligaments. The meniscus, cartilages components and other secondary ligaments and capsular soft tissues strengthen the whole structure whatever the loading conditions. This lower limb model mesh is much more accurate than other model usually used for crash simulations. The current mesh is accurate enough to give a good estimation of model response. Additionally, we performed parametric studies on the influence of mesh accuracy on the model response and showed that results could be improved through mesh refinements, in order to model the failure process. Besides, mesh refinement will substantially increase time calculations.

This model presents also limitations in terms of descriptions of mechanical properties of biological tissues. More particularly, the damage and unsymmetrical behaviour laws were not included in the model at this stage, which limits the model validity to the first ligament failure and muscle tone potential influence. These first results have to be improved with further developments, including damage and failure properties and also more accurate description of tissues viscoelastic properties. Coupled with large sensitivity study of the model it will be then possible to define a risk corridor for these ultimate levels.

Notes lastly that all runs were performed with a stable time step which ranged from $0.7\ 10^{-3}$ to $0.4\ 10^{-4}$ ms. Hourglass evolution was low (less than 15% of internal energy) and total error was lower than 8%.

5.2. *About the study of injury mechanisms and assumptions in injury criteria*

The results illustrate the ability of the model to describe such impact situations and to provide experimentally unavailable data.

For the bending test, the knee injury mechanism can be described as a lateral rotation around the contact area between the lateral femoral condyle and tibial glena. This rotation simultaneously induces a high deflection of both anterior cruciate and medial collateral ligaments, assumed to be injured for rotations over 15 and 20 °respectively. These results were not sensitive to impact velocities, and seem to be relevant with those experimentally identified at specific velocities. Then concerning injury criteria, as a conservative value, 15° of lateral rotation can be considered as a failure criterion for the ligaments in knee joint.

For pure shearing impacts, the chronology of ligament failure concerned the anterior, posterior cruciate and tibial collateral ligaments. The ultimate shearing level was computed by recording the distance between the tibial eminence and the condylar notch that reached up to 13 to 15 mm. Considering lateral shearing, the results were not sensitive to impact velocity and a conservative criteria would be to consider a lateral shearing of 13mm as a failure criteria for the knee joint in shearing.

For the pedestrian full scale impact, numerical simulation results were relevant with experiments. It showed that in this situation, the bending effects were dominant regarding to shearing effects. Considering failure criteria established for sub segment testing, the assumptions of ligaments injuries during the test were relevant with observations performed during post-crash necropsies.

For all the studied impact situations, the criteria postulated above were strongly dependant on the material properties (especially the postulated failure criteria). A further study including a damage model for tissues as well as a parametric study around the failure criteria should be performed in order not to summarize the injury criteria to a single couple of value (lateral rotation and shearing) but also to define injury risk curves.

The strain versus time curves show the influence of impact velocity and the time dependent answer of the whole structure which could be mainly attributed to structure effects and also soft tissue viscoelastic properties. It also underlines the differences in strain distribution between cruciates and collateral ligaments. For the cruciates ligaments, high strain levels were recorded on ligaments insertions (in agreement with experimental results), that underlines failure properties of cruciate ligaments at their insertions. 8 years ago, when we started studying behaviour laws of knee ligaments under dynamic loadings (Arnoux 2000, 2002, 2003), we assumed that ligaments loading velocity was around 2m/s for a which strain rate were closed to 5000 & 10000%/s , deduced on interpretations of sub segment testings (bending and shearing) but also on full scale experiments on pedestrians. Such strain rate levels were now evaluated quantitatively. It also shows strong dispersion between cruciate and lateral ligaments, as well as between the whole ligaments or locally. Such results seem to show that shearing effects seems to be more aggressive to the knee because of the high strain level induced.

Von Mises distribution was systematically located on the same metaphysis areas of the lower femur and upper tibia. This distribution could indicate a bending effect

on the two bones. It was also observed that for impact velocities over 10m/s, and according to the damping properties of the impacting surface, the failure risk for bones seems to be very high.

Concerning the kinematics aspects, whereas frontal flexion of the knee did not change significantly, torsion effects can not be neglected especially during the first phase of the impacts. This rotation, which could be attributed to the dissymmetry of the femoral condyles, was described as a safety countermeasure of the knee to avoid or limit ligament damage. Therefore, with numerical simulations, it was observed that even in pure loading, pure shearing or pure bending can not be obtained alone. The two mechanisms seem to be coupled with a majority of shearing or bending according to the loading conditions.

5.3. *Concluding remarks*

The lower leg model used in this study is an advanced FE model of the lower limb, validated under various situations (from physiological movements up to frontal and lateral impacts). Its accurate description of anatomical parts allows a wide range of use in this context.

According to the validity domain of the model in the context of lateral pedestrian impact, it offers a valuable tool for the numerical evaluation of injury mechanisms through data which can not be obtained experimentally. A risk criterion for knee ligaments was postulated through an ultimate bending of 15° and a shearing of 13mm. These injury criteria should now be checked and improved in order to be extended to other trauma situations.

Acknowledgment

We would like to acknowledge the technical staff of the laboratory which were in charge of experiments essential to the validation and evaluation of the numerical model. We would also acknowledge Mecalog for their close collaboration in the design of the lower limb model. Lastly we would like to acknowledge all partners of the PREDIT APPA project (Mecalog, Faurecia, INRETS MA, INRETS UMRETTE, UTAC and LAB PSA-Renault) for their contribution especially providing the numerical model of the car front.

6. References

Arnoux P.J., Modélisation des ligaments des membres porteurs, Ph D. Thesis, Université de la Méditerranée, 2000.

Arnoux P.J., Kang H. S., Kayvantash K., “The Radioss Human model for Safety”, *Archives of Physiology and Biochemistry*, vol. 109, 2001, p. 109.

Arnoux P.J., Cavallero C., Chabrand P., Brunet C., "Knee ligaments failure under dynamic loadings". *International Journal of Crashworthiness*, Vol 7 (3), 2002, pp. 255-268.

Arnoux P. J., Thollon L., Kayvantash K., Behr M., Cavallero C., Brunet C., "Advanced lower limb model with Radioss, application to frontal and lateral impact Radios lower limb model for safety", *Proceedings of the IRCOBI Conference*, 2002.

Arnoux P.J., Kang H.S., Kayvantash K., Brunet C., Cavallero C., Beillas P., Yang H., "The Radioss Lower Limb Model for safety: application to lateral impacts", *International Radioss user Conference*. Sophia, June 2001.

Arnoux P. J., Cesari D., Behr M., Thollon L., Brunet C., "Pedestrian lower limb injury criteria evaluation a finite element approach", under press in *Traffic Injury Prevention journal*, 2004.

Atkinson P., A stress based damage criterion to predict articular joint injury from subfracture insult, Ph.D. thesis, Michigan State University 1998.

Atkinson P.J., Haut R., Eusebi C., Maripudi V., Hill T., Sambatur K., "Development of injury criteria for human surrogates to address current trends in knee-to-instrument panel injury", *Stapp Car Crash Conference Proceedings*, pp. 13-28, 1998.

Attarian D.E., Mc. Crackin H.J., Mc. Elhaney J.H., DeVito D.P., Garrett W.E., "Biomechanics characteristics of the human ankle ligaments", *Foot and Ankle*, vol. 6., N°. 2, pp. 54-58, 1985.

Banglmaier, R.F., Dvoracek-Driskna, D., Oniang'o, T.E., and Haut, R.C. "Axial compressive load response of the 90 degrees flexed human tibio femoral joint", *43rd Stapp Car Crash Conf. Proceedings.* 1999, pp. 127-138.

Beaugonin M., Haug E., Cesari D., "A numerical model of the human ankle/foot under impact loading in inversion and eversion", *40th Stapp Car Crash Conference Proc.*, 1996.

Beaugonin M., Haug E., Cesari D., "Improvement of numerical ankle/foot model: modeling of deformable bone", *41th Stapp Car Crash Conference Proc.*, 1997.

Bedewi P.G., Bedewi N.E., "Modelling of occupant biomechanics with emphasis on the analysis of lower extremitiey injuries", *International Journal of Crash*, Vol. (1): p. 50-72, 1996.

Behr M., Arnoux P. J., Serre T., Bidal S., Kang H.S., Thollon L., Cavallero C., Kayvantash K., Brunet C., "A Human model for Road Safety : From geometrical acquisition to Model Validation with Radioss", *International Journal on Computer Methods in Biomechanics and Biomedical Engineering*, vol 6, No. 4, 2003.

Behr M., Arnoux P.J., Thollon L., Serre T., Cavallero C., Brunet C., "Towards integration of muscle tone in lower limbs subjectes to impacts", *IX International Symposium on Computer Simulation in Biomechanics*, Juin 2003, Sydney, Australia.

Beillas P., Arnoux P. J., Brunet C., Begeman P., Cavallero C., Yang K., King A., Kang H. S., Kayvantash K., Prasad P., "Lower Limb: Advanced FE Model and New Experimental Data", *International Journal of STAPP - ASME*, vol. 45, pp. 469-493, 2001.

Beillas P., Modélisation des membres inférieurs en situation de choc automobile, Ph.D. thesis, Ecole Nationale Supérieure d'Arts et Métiers, Paris, France, 1999.

Beillas P., Lavaste F., Nicoloupoulos D., Kayventash K., Yang K. H., Robin S., "Foot and ankle finite element modeling using CT-scan data", *Stapp Car Crash Conference Proc.* 1999.

Bennett, M.B. and Ker, R.F., "The mechanical properties of the human subcalcaneal fat pad in compression". *J. of Anat*., 171, p.131-138, 1990.

Bidal S., Reconstruction tridimensionnelle d'éléments anatomique et génération automatique de maillages éléments finis optimisés, PhD. Thesis, Université de Provence, 2003.

Bose D., Bhalla K., Rooij L., Millington S., Studley A., Crandall J., "Response of the Knee joint to the pedestrian impact loading environment", *SAE World Congress*, 2004.

Burstein A.H., Currey J.D., Frankel V.H., Reilly D.T., "The ultimate properties of bone tissue: the effects of yielding", *J. of Biomech*., p. 35, 1972.

Chawla A., Mukherjee S., Mohan D., Parihar A., "Validation of Lower Extremity Model in THUMS", *IRCOBI conference*, 2004.

Crandall J.R., Portier L., Petit P., Hall G.W., Bass C.R., Klopp G.S., Hurwitz S., Pilkey W.D., Trosseille X., Tarriere C., and Lassau J.P., "Biomechanical response and physical properties of the leg, foot, and ankle", *40th Stapp Car Crash Conference Proc.* SAE, pp. 173-192, 1996.

Goldstein S.A., "The mechanical properties of trabecular bone: dependence on anatomic location and function", *Journal of Biomechanics*. Vol. 20, (11.12), p. 1055-1061, 1987.

Grzegorz Teresinski, Roman Madro, "Pelvis and hip injuries as a reconstructive factors in car-to-pedestrian accidents", *Forensic Science International* 124, pp 68-73, 2001.

Haut R. C., Atkinson P. J., "Insult to the human cadaver patellofemoral joint : effect of age on fracture tolerence and occult injury", *39th Stapp Car Crash Conference Proc.*, SAE, 1995.

Hayashi S., Choi H.Y., Levine R.S., Yang K.H., King A.I., "Experimental and analytical study of knee fracture mechanisms in a frontal knee impact", *40th Stapp Car Crash Conf. Proc.*, p. 161, 1996.

IHRA/PS/200, International Harmonized Research Activities, Pedestrian Safety Working Group Report, 2001.

Johnson G.A., "A single integral finite strain viscoelastic model of ligaments and tendons." *J. of Biomech. Eng.*, vol. 118, pp. 221-226, 1996.

Kajzer J., Cavallero C., Bonnoit J., Morjane A., Ghanouchi S., "Response of the knee joint in lateral impact: Effect of bending moment", *Proc. IRCOBI*, pp. 105-116, 1993.

Kajzer J., Cavallero C., Bonnoit J., Morjane A., Ghanouchi S., "Response of the knee joint in lateral impact: Effect of shearing loads", *Proc. IRCOBY*, pp. 293-304, 1990.

Kennedy J.C., Weinberg H.W., Wilson A.S., "The anatomie and function of the anterior cruciate ligament", *J. Bone Joint Surg.*, vol. 56, pp. 223-235, 1974.

Kerrigan J.R., Ivarsson B.J., Bose D., Madeley N.J., Millington S.A., Bhalla K. S., Crandall J.R., "Rate sensitive constitutive and failure properties of human collateral knee ligaments", *IRCOBI conference*, pp. 193, 2003.

Li L.P., Buschmann M.D., Shirazi-Adl A., "Stain rate depedent stiffness of articular cartilage in unconfined compression", *Journal of Biomechanical Engineering*, Vol. 125, pp. 161-168, 2003.

Lizee E., Robin S., Soong E., Bertholon N., Le Coz J. Y., Besnault B., Lavaste F., "Developpement of a 3D finite element model of the human body", *Proc. Stapp Car Crash Conf.*, pp. 215-238, 1998.

Marinozzi G., Pappalardo S., Steindler R., "Human knee ligaments: mechanical tests and ultrastructural observations". *Ital. J. Orthop. Traum.*, Vol. 9, pp. 231-240, 1982.

Mcelhaney J.H., "Dynamic response of bone and muscle tissue", *J. Appl. Physiol*, 21(4): pp. 1231-1236, 1966.

Mow V.C., Kuei S.C., Lai W.M., Holmes M.H., "Biphasic creep and stress relaxation of articular cartilage in compression. Theory and experiment", *Journal of Biomechanical engineering*, 102, 1980, pp. 73-84.

Noyes F.R., "The strength of the anterior cruciate ligament in humans and rhesus monkeys", *J. of Bone & Joint Surgery*, pp. 1074-1081, 1976.

Nyquist G.W., Cheng R., El-Bohy A.R., King A.I.. "Tibia bending : strength and response", *29th Stapp Car Crash Conference Proc.*, pp. 99-112, SAE, 1985.

Parenteau C.S., Foot and Ankle joint response – epidemiology, biomechanics and mathematical modeling, Ph. D. thesis, Chalmers Univ. 1996.

Prietto M.P., Bain J.R., Stonebrook S.N., Settleage R.A., "Tensile strength of the human posterior cruciate ligament (PCL)", *Trans. Orthop. Res. Soc.*, vol. 17, pp. 124, 1992.

Race A., "The mechanical properties of the two bundles of the human posterior cruciate ligament", *J. Biomech.*, vol 9, pp. 449-452, 1976.

Radin E.L., Paul I.L., Lowy M., "A comparison of the dynamic force transmitting properties in subchondral bone and articular cartilage", *Journal of Bone and Joint Surgery*, 52A, 1970, 444-456.

Reilly D.T., Burstein A.H., "The elastic and ultimate properties of compact bone tissue", *Journal of Biomechanics*, p. 393, 1975.

Repo, R. and Finlay, J., "Survival of articular cartilage after controlled impact", *Journal of Bone Joint and Surgery*, (59), 1977, pp. 1068.

Schuster P.J., Chou C.C., Prasad P., Jayaraman G., "Development and Validation of a Pedestrian Lower Limb Non-Linear 3-D Finite Element Model", *44th Stapp Car Crash Conference Proceedings*, Atlanta, 2000-01-SC21, 2000.

Stutts J.C., Hunter, W.W., "Motor vehicle and roadway factors in pedestrian and bicyclists injuries: an examination based on emergency department data", *Accident analysis and prevention*, Volume 31, No 5, 1999, pp. 505-514.

Subit D., Modélisation de la liaison os ligament dans l'articulation du genou, PhD. Thesis, Université de la Méditerranée, 2004.

Tannous R.E., Bandak F.A., Toridis T.G., Eppinger R.H., "A three-dimensional finite element model of the human ankle: development and preliminary application to axial impulsive loading", *40th Stapp Car Crash Conference Proc.*, SAE. pp. 219-238, 1996.

Thollon L., Modélisation du membre thoracique dans le cadre d'un choc latéral: Approche expérimentale et numérique, Ph. D. Thesis, Université de la Méditerranée, 2001.

Thollon L., Arnoux P. J., Kayvantash K., Cavallero C., Brunet C., "From dummy criteria to injury evaluation using Humos Radioss finite element model", *Proceedings of the IRCOBI conference*, 2002.

Tropiano P., Thollon L., Arnoux P.J., Behr M., Kayvantash K., Brunet C., Finite element analysis and virtual traumatology : Application to Neck-injury in frontal crash situations, *Spine*, Vol. 29, N°16, 2004, pp. 1709-1716.

Viano D.C., Culver C.C., Haut R.C., Melvin J.W., Bender M., Culver R.H., Levine R.S., "Bolster impacts to the knee and tibia of human cadavers and an anthropomorphic dummy", *22nd Stapp Car Crash Conference Proc*., 1978, pp. 401.

Viidick A., "Functional properties of collagenous tissues", *Int. Rev. of connective tissue research*, Vol 6, Academic press, New York, 1973.

Yamada H, *Strength of biological matérials*, Edited by F. Gaynor Evans, 1970.

Yang J., Injury Biomechanics in car pedestrian collisions: development, validation and application of Human-Body mathematical models, Ph.D. thesis, Chalmers University 1997.

Appendix 1. Overview of knee joint mesh

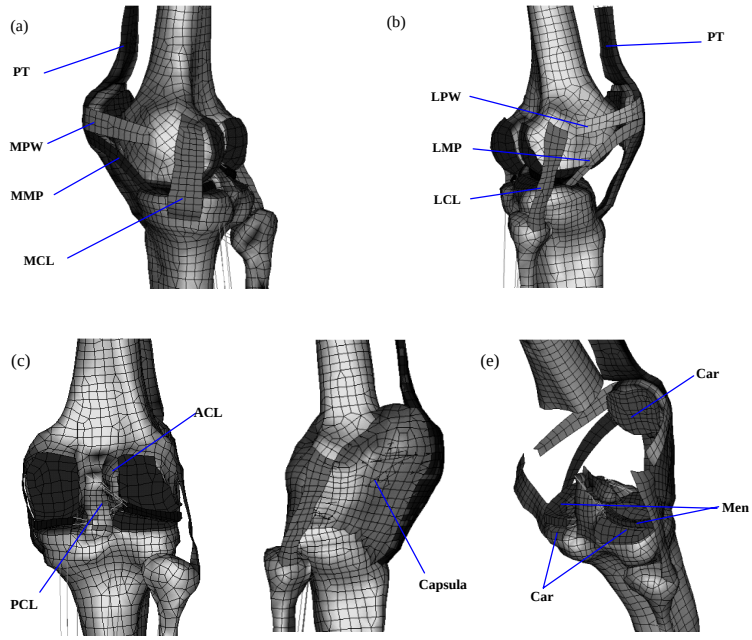

Figure 1. *Overview of knee joint meshes*

Medial (a), tibial (b), posterior (c), with capsula (d) and opened view (e) of the knee model. On the medial and tibial view, the Medial and Lateral Collateral Ligaments (MCL and LCL), the medial and lateral patellar wing (MPW and LPW), the medial and lateral meniscus patellar ligaments (MMP and LMP)and the patellar tendon (PT) can be shown. On the posterior view, the two cruciate ligaments (ACL and PCL) can be identified but also spring elements which modeled meniscus to femur and tibia attachment. On the last view, distal femur and femur cartilage was removed in order to show cartilage (Car) and meniscus (Men) components

Appendix 2. *Overview of model validation database*

	COMPUTED DATA	**Reference**
ISOLATED MATERIAL		
Anterior Cruciate traction	Force, Displacement	Arnoux 2000
Posterior Cruciate traction	Force, Displacement	Arnoux 2000
Medial collateral liagment traction	Force,Displacement	Arnoux 2000
Tibial collateral liagment traction	Force, Displacement	Arnoux 2000
Three point femur bending	Force, Displacement	Beillas 1999
Patellar tendon traction	Stress, Strain	Johnson 1996
SUB-SEGMENT TESTS		
Knee joint Kinematic		
Haut patellar impact on flexd knee	Force, time	Haut 1995
Hayashi patellar impact on flexed knee	Force, time	Hayashi 1996
Banglmeier Tibia impact on flexed knee	Force, time	Banglmeier 1999
Antero-posterior flexed knee loading	Force, Displacement	Viano 1978
Tibia Latero-medial 3 point bending	Force, time	Nyquist 1985
Tibia antero-posterior 3 point bending	Force, time	Nyquist 1985
Quasi-static lower leg compression	Force, displacement	Bennet 1990
Quasi-static tibo-fibular compression	Force, displacement	Beillas 2001
Ankle Inversion	Moment, rotation	Parenteau 1996
Ankle Eversion	Moment, rotation	Parenteau 1996
Ankle dorsiflexion	Moment, rotation	Parenteau 1996
WHOLE LLMS MODEL		
Pedestrian LBA lateral bending	Force, Rotation	Kajzer 1993
Pedestrian LBA lateral shearing	Force, time	Kajzer 1990
Frontal Wayne sled test	Force, time	Beillas 2001